

# Analysis of Spacecraft Anomalies due to the Radiation Environment

M. Lauriente\*

NASA Goddard Space Flight Center, Greenbelt, Maryland 20771

A. L. Vampola†

University Research Foundation, Greenbelt, Maryland 20771

and

R. Koga‡ and R. Hosken§

The Aerospace Corporation, El Segundo, California 90245

**Various space-environment-induced anomalies are discussed and new tools under development are demonstrated that are now or soon will be available to the spacecraft designer to mitigate the effects of the space environment on space systems. Two-dimensional cross correlations between spacecraft anomalies and trapped particle models provide information on the energy of the particles that cause the anomalies and are also used to evaluate the accuracy of energetic proton models. Results of studies using anomalies and background effects in satellite sensors to evaluate the AP8 trapped radiation model and an update to it are also presented.**

## Introduction

ENERGETIC trapped particles and cosmic rays pose a serious hazard to spacecraft because a single particle can cause a malfunction in components such as random access memories, microprocessors, hexfet power transistors, etc., through the creation of electron-hole pairs in a sensitive volume within a device. The electron-hole pairs constitute a signal that can turn on junctions, including volumes of a device that are not intended to be active and are not normally connected to any circuitry (phantom transistors). Such malfunctions are called single-event effects (SEEs). SEEs are usually separated by the type of effect: single-event upset (SEU), which is a reversible change in the state of a digital circuit; single-event latchup, which is a change in state that requires interruption of power to the device or other action to restore it to its former (or correct) state; and single-event burnout, in which the device failure is nonreversible. Cosmic rays and energetic trapped particles can also generate background noise in star sensors, infrared detectors, and charge-coupled devices. In addition to noise, these energy deposits can masquerade as real signals, which may affect subsystems.

When SEEs occur on newly launched satellites, there is always an intense investigation to determine the exact mechanism involved in the SEEs to alleviate the occurrence of such SEEs in the future and to provide a basis for future designs that will be less susceptible to SEEs. The cross-correlation technique discussed in this paper permits the identification of the threshold energy required for protons to produce the SEEs, even when the proton models have limited accuracy. We demonstrate the use of this cross-correlation technique on several different classes of SEEs, and also show that the technique is even applicable to examination of the particle environment itself.

We are concerned primarily with the particle environment that causes these various effects, rather than the effects themselves, so we will ignore the subclasses and use the generic SEE. We will discuss a two-dimensional cross-correlation technique that can identify the

energy threshold of the protons that produced the anomalies and background effects.

## Cross Correlations with Trapped Radiation

Trapped radiation belts have been recognized as a hazard to space flight since they were first discovered by Van Allen in 1958.<sup>1</sup> They consist of electrons and protons (with a few alphas and a negligible number of heavier particles) and are distributed nonuniformly within the magnetosphere. The currently used trapped proton models are AP8MIN and AP8MAX, which represent the solar minimum and maximum periods. At solar maximum, the increased atmospheric scale height results in a decrease of the proton fluxes at low altitudes. This decrease is observable in the distribution of SEEs on low-altitude satellites. A history of the development of the NASA standard electron and proton models, AE8 and AP8, is given by Gaffey and Belitza.<sup>2</sup>

There has been concern about the geographic accuracy of energetic proton flux predictions at near-Earth altitude, such as for the Shuttle or space station, that are obtained from AP8 because of secular changes in the magnetic field that have occurred since the AP8 model was created.<sup>3</sup> The error in predicting present or future particle distributions, which is based on a trapped particle model defined by an earlier magnetic field epoch, for example, International Geomagnetic Reference Field 65 (IGRF65), epoch 1970 for AP8MAX, has been analyzed theoretically by Lemaire et al.<sup>4</sup> The secular decrease in the dipole term of the Earth's magnetic field results in a westward and southward drift of the ground-level local minimum in the magnetic field known as the south atlantic anomaly (SAA). The low-altitude peak in proton flux intensity moves westward and slightly northward.<sup>5</sup> The reason it moves northward is that the magnetic field configuration is changing (not moving like a rigid structure), and the change in the field minimum at the altitudes of interest to low-altitude satellites results in the particle ensemble maximum being observed at a westward and northward location. The location of the centroid of the proton flux pattern at low altitude is a function of the proton energy. Lower energy protons are observed farther south (higher  $L$ ) and farther east (lower atmospheric density required to absorb them). The apparent motion of the pattern of proton intensities is a function of both energy and altitude. The cross-correlation technique that we use establishes the present location of the proton SAA by analyzing the SEEs produced in low-altitude satellites by those protons.

## Cross-Correlation Method

Our approach in investigating low-altitude proton-induced SEEs is to use a two-dimensional (longitude and latitude) cross correlation

Presented as Paper 98-1048 at the AIAA 36th Aerospace Sciences Meeting, Reno, NV, 12–15 January 1998; received 27 March 1998; revision received 9 September 1998; accepted for publication 28 April 1999. Copyright © 1999 by the American Institute of Aeronautics and Astronautics, Inc. No copyright is asserted in the United States under Title 17, U.S. Code. The U.S. Government has a royalty-free license to exercise all rights under the copyright claimed herein for Governmental purposes. All other rights are reserved by the copyright owner.

\*Manager, EnviroNET, Code 730. Member AIAA.

†Consultant; retired. Associate Fellow AIAA.

‡Senior Scientist, Space Sciences Department.

§Engineering Specialist, Computer Systems Department.

between the SEE data set and the current-epoch AP8 predicted fluxes. We quantitatively compare (correlate) the area distributions of the SEEs with the area distributions of the protons. The correlation must be done as a function of proton energy and satellite altitude because, at a given longitude and latitude, the proton flux intensity varies with both energy and altitude. Furthermore, because the magnetic field is not a uniform dipole, at a given proton energy or orbit altitude, the flux intensity varies as a function of longitude and latitude. In performing the correlation, it is not necessary that the particle energy threshold for production of the SEE be known because the analysis provides it.

The current-epoch AP8 model that we use is a modification of the AP8 model in which  $B$  and  $L$  for a location in space are calculated using the IGRF magnetic field epoch for the period during which the SEEs occur. Under normal usage of AP8, the  $B$  and  $L$  are calculated using a hybrid magnetic field model that is (apparently) a proposed IGRF65 (Ref. 6) using a mid-1950s dipole moment (0.31165 g). Because of the secular variation in the Earth's magnetic field, AP8 is conceded to be inaccurate at low altitude. The model makes no provision for a changing magnetic field. Further, the location of the energetic proton SAA has moved westward and slightly northward since AP8 was generated. In Ref. 5, we intercompared the low-altitude magnetic field configurations in the SAA using the IGRF70 model with the preceding magnetic field model as originally distributed by the National Space Science Data Center with the ORB software.<sup>7</sup> At 1336 we found an offset of about 0.25 deg between the two magnetic field models.<sup>5</sup> This offset is used to correct all of our calculations using the IGRF series of models. Note that this approach, using a current-epoch magnetic field model with AP8, produces correct geometric patterns (relative intensity vs longitude, latitude, and altitude) but does not produce a quantitatively correct flux value. Hence, it cannot be used to evaluate ground-based linear energy transfer (LET) test data or on-orbit upset rate predictions.

A contour plot of the energetic proton flux at constant altitude as predicted by AP8 results in a highly asymmetric pattern. This is the result of the asymmetric geomagnetic field. If we have a large database of events that are geographically spaced and are probably caused by these energetic protons, we can determine quantitatively the relationship between the two geographic distributions, if there is one.

As an example of the use of this technique, we start with a geographical distribution of anomalous events in the TOPEX/Poseidon Earth sensors. The TOPEX/Poseidon satellite was launched 10 August 1992 into a circular Earth orbit at an inclination of 66 deg and an altitude of 1336 km. In this orbit, the satellite traversed the SAA region approximately six times per day. A total of 2172 Earth sensor anomalies were experienced between launch and mid-1994. The anomalies occurred in two Earth sensor assemblies located in the module on the Earth-facing side of the spacecraft.

The cross-correlation analysis uses the anomalies and the AP8 proton model. The anomaly database is geographically limited, but the AP8 model is not. We generate a normalized grid of AP8 proton flux intensities  $P_{ij}$  at the altitude of TOPEX at  $0.5^\circ \times 0.5^\circ$  longitude-latitude intervals from  $-150^\circ$  to  $+70^\circ$  in longitude and  $-70^\circ$  to  $+40^\circ$  in latitude. The anomalies are used to produce a similar normalized grid  $A_{kl}$ , from  $-120^\circ$  to  $+50^\circ$  in longitude and  $-50^\circ$  to  $+20^\circ$  in latitude, in which the elements of this grid are the number of anomalies that have occurred in that bin. They are binned into  $0.5^\circ \times 0.5^\circ$  longitude-latitude bins. This is a sparse data set. On average, only 1 out of each 22 bins contains an event. However, the large number of events allows for determining the centroid of the distribution to fairly high accuracy.

The anomaly grid  $A_{kl}$  is then offset with respect to the proton grid  $P_{ij}$  by  $-20^\circ$  in both longitude and latitude, and the sum  $\sum A \cdot P$  (the sum of element-by-element products over the entire  $A$  grid) is generated. The  $A$  grid is then shifted by one element ( $0.5^\circ$ ) in longitude or latitude. In this way, a correlation grid is produced,  $C_{mn}$ , in which each element is the sum of the products  $A_{rs} \cdot P_{rs}$  where  $m$  and  $n$  are indexed  $\pm 20^\circ$  by shifting the  $A$  grid by one element ( $0.5^\circ$ ) in either latitude or longitude and  $r, s$  cover the parameter space from  $-120^\circ$  to  $+50^\circ$  longitude and  $-50^\circ$  to  $+20^\circ$  latitude at  $0.5^\circ$  increments. The  $C$  array is then normalized, and a contour plot is made of the correlation strengths. Figure 1 is such a plot, where

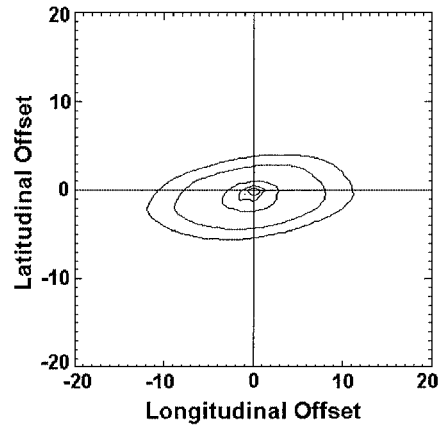


Fig. 1 Cross correlation of AP8MIN 80 MeV protons and SEEs on TOPEX.

the  $P$  grid was generated using the AP8MAX  $> 80$  MeV protons at 1336 km and the  $A$  grid was generated from the TOPEX anomalies. The highest correlation strength occurs with essentially no offset in either latitude or longitude, indicating that the centroids of the two distributions (the  $A$  and  $P$  arrays) coincide.

If we do the described procedure with lower energy protons, we get a maximum correlation with an offset that is in the lower right quadrant of the contour plot, which is to be expected because the lower energy protons have their maximum flux at higher  $L$  (farther away from the equator) and are absorbed at lower atmospheric densities along their drift paths, which occur to the east. Higher energy protons maximize closer to the equator and farther west. By cross correlating a set of SEEs with increasing proton energies, one gets a pattern in correlation peaks that starts in the lower right quadrant in a plot like Fig. 1 and progresses to the upper left quadrant. Under ideal conditions, the correlation pattern goes through zero offset in both longitude and latitude at the same time, enabling one to unambiguously identify the threshold proton energy for production of the SEEs. Cross-correlating the TOPEX anomalies with a series of AP8MAX proton energy grids at the TOPEX altitude produces the results seen in Fig. 2. The offsets shown in Figs. 1 and 2 have been corrected for the 0.25° offset in latitude that exists between the actual DGRF65 epoch 1970 and the pseudo-IGRF65 epoch 1970 that was used for AP8MAX. The offset was determined by cross correlating grids of the magnetic field intensities from the two models at the TOPEX altitude.<sup>5</sup> The centroid of the TOPEX SEEs coincided with the AP8MAX epoch 1993.5 predicted maximum of  $> 80$  MeV protons and above within an accuracy of  $\sim 0.2^\circ$  (Fig. 1). It is obvious from Fig. 2 that these SEEs are caused by protons  $> 80$  MeV (which is why we used the 80 MeV proton correlation for the example in Fig. 1).

The same procedure was used with a subset of the TOPEX SEEs: errors in the pitch-roll assembly. In this case, the particles causing the errors were much more energetic than in the preceding case. The threshold for production of these errors was about 175 MeV. The difference between the two types of anomalies may be due to differences in the thickness of matter that the protons must penetrate to get to the sensitive volume. This cross-correlation technique shows that using AP8 with a present-epoch magnetic field model accurately predicts the present location of the SAA proton flux enhancement at the TOPEX.<sup>5</sup>

The approach used here is not novel. However, in previous computing environments (when the mainframe computer was the only choice available), such a procedure would have been prohibitively expensive. In our case, with  $A$  containing a matrix of  $(\text{long./Dlong.}) \times (\text{lat./Dlat.}) = 341 \times 141$  elements, each  $C_{mn}$  is the sum of 48,081 products. The  $A$  grid is offset in  $81 \times 81$  positions ( $\pm 20^\circ$  in longitude and latitude at  $0.5^\circ$  intervals) = 6561C elements. The total number of floating-point mathematical operations,  $> 6 \times 10^8$  per  $C$  grid, is trivial in today's computing environment. The three arrays,  $A$ ,  $P$ , and  $C$ , can be generated on a 200-MHz Pentium processor in a little over 1 min, most of which is spent calculating the  $C$  array. The total number of floating-point calculations

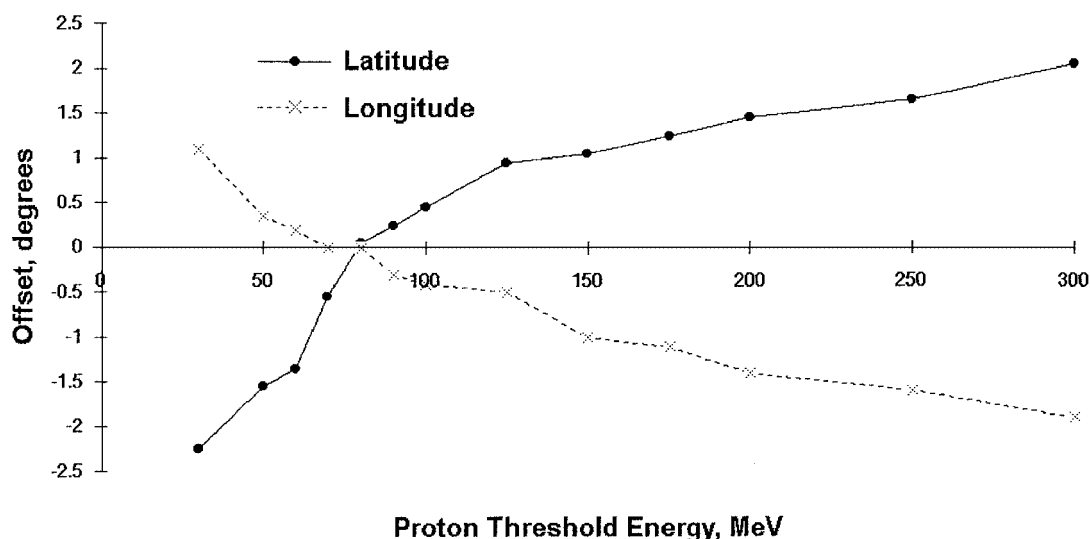


Fig. 2 Cross correlation of the TOPEX SEEs with the AP8MIN proton model at various threshold energies.

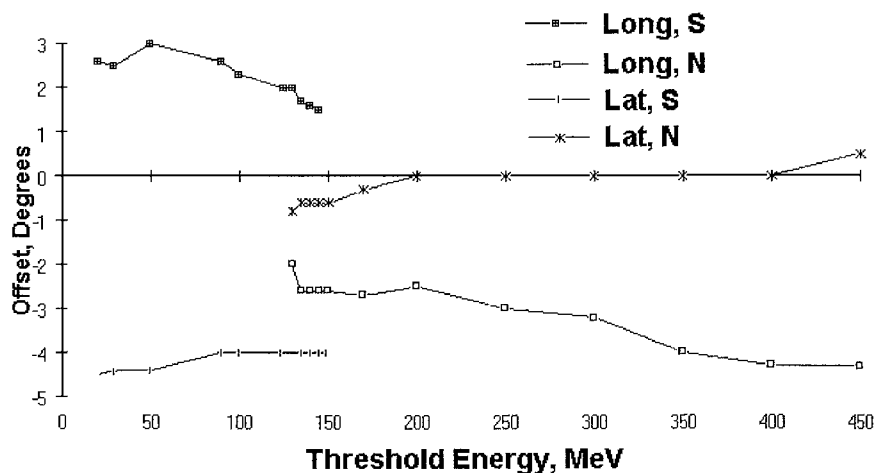


Fig. 3 Cross correlation of COBE/DIRBE sensor noise with AP8MIN at 890 km.

required to produce Fig. 2 was in excess of  $10^{10}$  but required less than 2 h of personal computer time.

### Cosmic Background Explorer Noise vs Proton Energy Threshold

This correlation method was also used for instances of excess noise in the cosmic background explorer (COBE)/DIRBE sensor, which was designed to look at the cosmological infrared (IR) continuum from the big bang theory and at other IR sources. Because COBE was at a lower altitude than TOPEX, this gave us a second cut at the present distribution of energetic protons in the SAA. COBE is in a high-inclination 890-km circular orbit. The DIRBE sensor consists of a set of IR detectors at several wavelengths. During passage through the SAA or the low-altitude extensions of the outer zone electron belts, a shutter of several grams per square centimeter is used to protect the detectors. Excess signal in a detector for a single count cycle was considered to be due to particle penetration.

The data were stored in 128-s segments, so that there was an uncertainty in the location of a glitch of about  $\pm 3^\circ$  along the orbit path. This uncertainty smears the data set for correlation purposes, but the two-dimensional correlation method locates the centroid of the distribution. A large data set provides accurate results if there are enough samples. This time a problem with the proton model surfaced. Figure 3, the result of an energy-dependent analysis similar to that shown in Fig. 2, shows a discontinuity in the location of the peak correlation. The discontinuity is actually produced by a dual-peaked intensity structure found above 100 MeV in AP8 at  $\sim 900$  km. This is an artifact of the model. The cause of the background in the

DIRBE detectors was determined by this analysis to be protons with energies of 200 MeV or above that penetrated the thick shutter.<sup>8</sup>

### Solar Cycle Variations in Trapped Protons

The variation in scale height of the atmosphere due to the variation in solar EUV as a function of solar cycle should produce a change in the trapped energetic proton population in the inner zone. At solar minimum, the protons diffuse to lower altitudes before being absorbed by the atmosphere because the effective top of the atmosphere is lower. The lower height translates to a lower  $L$  value, which in turn translates to a northward change in the location at which the peak proton flux should be observed.

This effect was demonstrated<sup>9</sup> by using SEE data from the total ozone mapping spectrometer (TOMS) instrument on a Meteor-3 spacecraft that was flown from mid-1991 (less than a year after solar maximum) through early 1995 (about a year prior to solar minimum). This flight at 1200 km, 82.5-deg inclination, contained a 128-Mbit solid state recorder that was subjected to proton induced errors. The number of errors were recorded at 128-s intervals and were telemetered. During this period the centroid of the anomalies moved  $2.6^\circ$  northward. Figure 4 is a contour map of the cross correlation of six months of SEE data starting with launch in 1991 with six months of data early in 1995. This motion toward the equator represents a lowering in  $L$  of the center of the energetic proton distribution. The  $2.6^\circ$  change in latitude corresponds to  $\Delta L \sim 0.03$  (from about 1.29 to 1.26). This translates to an average decrease in altitude of about 250 km in the energetic proton distribution at the equator, symbolic of the change in scale height of the Earth's atmosphere.

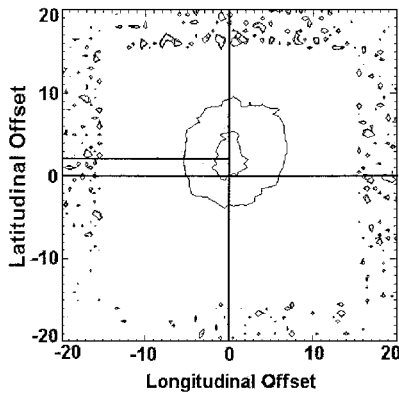


Fig. 4 Change in location of TOMS SEUs between 1991 and 1995.

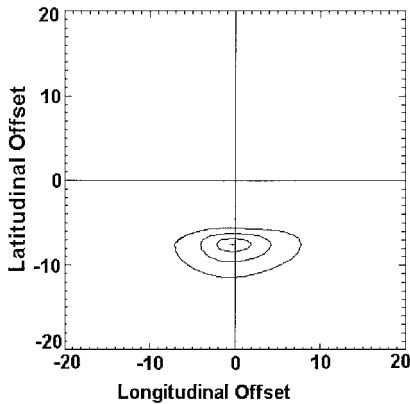


Fig. 5 Correlation of HST SEEs and the NOAA PRO 80–215 MeV low-altitude proton model.

### Solar Cycle Variations at Low Altitude

For this analysis, anomaly data from the TOMS-Earth probe satellite,<sup>9</sup> launched on 2 July 1996, at 500-km altitude was used. This is much lower than the altitudes of the satellites discussed earlier and should show gross changes in the proton environment at low altitude. In this case, we correlated the SEEs with the AP8MIN model. No change in latitude offset with proton energy was found, whereas there was a change in longitude. This latitudinal invariance is interpreted as an indication that at 500 km in the AP8MIN model the  $L$  profile is independent of energy. In corroboration, when one cross correlates the AP8MIN model with the AP8MAX model, no variation in longitude as a function of energy is seen. At 500 km, almost no variation in latitude is seen below 100 MeV and none above. Correlations with SEEs on the Hubble Space Telescope (HST) show an error in longitude for the AP8MIN model at low altitude.<sup>9</sup>

Data from the North Atlantic Oceanic and Atmospheric Administration (NOAA) TIROS-N weather satellite at 860 km have been collected for more than a solar cycle.<sup>10</sup> Data from the omnidirectional proton sensors were correlated for magnetic field model and time-tagging errors and were organized in terms of the average column density of residual atmosphere along their drift path. The solar variation in the  $F_{10.7}$  index is used as a proxy for the solar cycle variation in scale height of the Earth's atmosphere. The study has produced a new proton model called NOAA PRO for the region below 860 km for three energy ranges: 16–36, 36–80, and 80–215 MeV. It is organized in terms of  $L$ ,  $B/B_{min}$ , and  $F_{10.7}$ . The model was validated by cross correlation of HST anomaly data (623-km altitude orbit) with the 80–215 MeV map.<sup>11</sup> Figure 5 shows the NOAA PRO/HST SEE correlation. The longitudinal offset of a small fraction of a degree shows that the NOAA PRO model correctly predicts the westward shift of the energetic proton distribution at low altitude during solar minimum. The latitudinal offset is an artifact of the orbit that never sees the peak of the SAA because the peak is southward of  $-28.5^\circ$  (the inclination of the HST orbit).

The NOAA PRO model correctly predicted a solar-cycle-associated westward shift for the location of the SAA. The model also verified that proton flux at constant energy vs atmospheric den-

sity fit on the same curve without regard to solar cycle. However, the atmospheric density varies as a function of altitude and solar cycle, but not smoothly. Cross correlation of the HST SEEs with the AP8MIN indicated that the threshold proton energy for producing SEEs is probably between 125 and 275 MeV.

### Identification of an SEE Mechanism

The Technology Autonomous Operational Survivability (TAOS) satellite was launched on 13 March 1994 into a 550-km altitude, 105-deg inclined orbit<sup>12,13</sup> to test future Air Force systems in space. Two computers were monitored over three years. SEUs in 32 Kx8 static RAM chips were characterized. The two computers were identical in hardware and default software. One managed the bus and the other performed the computations of an experimental navigation system, the Microcosm Autonomous Navigation system.<sup>14</sup>

Both computers were instrumented with a program to monitor and transmit the computer status. This program functions all of the time while the other application programs are running and every 128 s takes an instantaneous sample of the bit errors recorded by the operating system. The operating system uses a scrubber to prevent the occurrence of a second SEE in a memory word that has already experienced 1-bit upset.

Examination of a 1296 SEE sample from one computer shows that 47% occurred in the SAA, whereas only 5% of the orbital time is spent in the SAA. The geographical distribution is shown in Fig. 6. The one sigma in-track error is approximately 3 deg due to the discrete time tag.

For the cross correlation with AP8MIN, only the SEUs represented by black squares were used. The others (and perhaps some of these) were produced by cosmic rays. The elements in which the SEUs occurred were relatively immune to upsets by low LET particles, such as protons. The cross correlation (Fig. 7) discloses the actual cause of the proton-induced SEUs. The correlation plot, which has an artificial offset due to the low-altitude errors in AP8MIN, indicates that protons with energies  $> 200$  MeV, or perhaps  $> 350$  MeV, are required to produce these upsets.

The cross correlation between the NOAA PRO proton model and the TAOS SEEs is also shown in Fig. 7. Note that because protons in our NOAA PRO model are 80–215 MeV protons, most of the protons in it are actually in the range of about 80–95 MeV. The NOAA PRO–TAOS SEE correlation point falls precisely on the AP8MIN correlation curve. Because the SEEs are caused by much higher energy protons, we see a large offset ( $\sim 4.5^\circ$ ) in longitude (reflecting the significant difference in energy, higher energy protons peak farther west). The NOAA PRO–TAOS SEE latitude correlation shows an offset because of the energy range of the NOAA PRO model compared to the energy of the particles causing the SEEs. AP8MIN fails to properly characterize the  $L$  dependency of protons as a function of energy at low altitude, resulting in a more or less constant latitude offset.

These protons have sufficient energy to produce nuclear interactions (Fig. 8). The result of a nuclear interaction is the deposition of a large amount of energy in the vicinity of the interaction and the

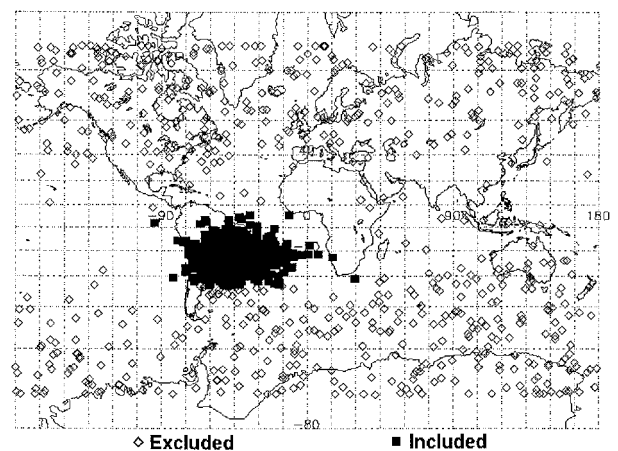


Fig. 6 SEEs observed in the TAOS satellite.

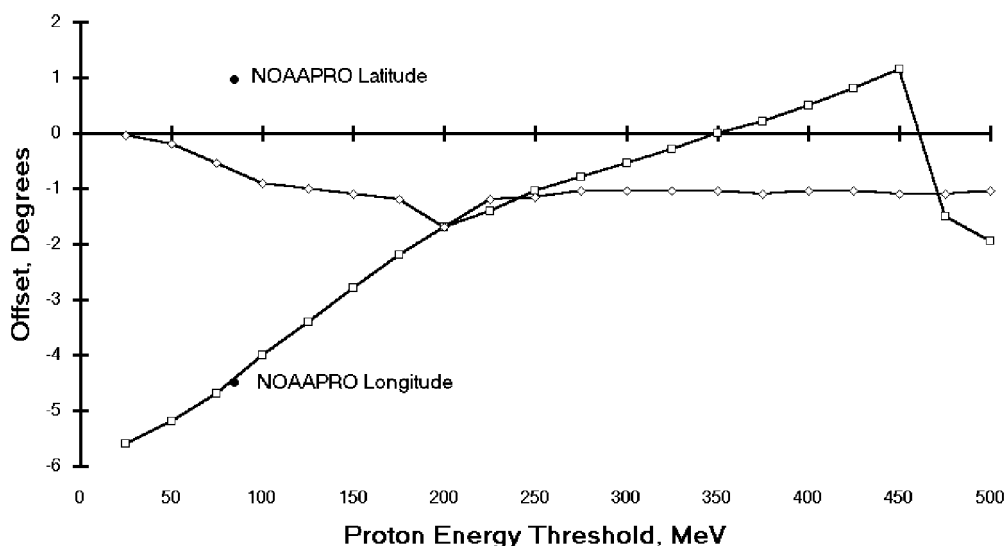


Fig. 7 Correlation of TAOS SEEs and AP8.

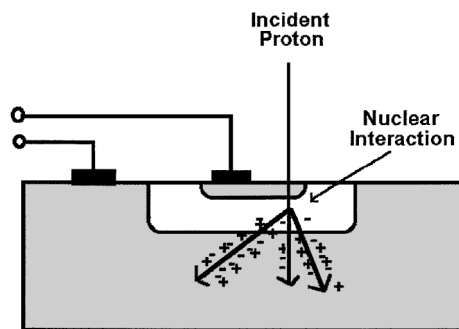


Fig. 8 Mechanism by which proton-induced nuclear interactions produce SEEs in radiation-tolerant devices.

production of high LET heavy ions, resulting in upsets in chips that are designed to be immune to low LET particles.

### Conclusion

We have presented examples of correlations between magnetospherically trapped particle environments and SEEs on various satellites. We have also presented examples of the use of a powerful new tool, two-dimensional cross correlations, that has been used to determine the energy of particles producing SEEs, address the accuracy of particle models, and even indicate the mechanism of a particular subset of SEEs. Our demonstration that use of a present epoch magnetic field model with the AP8 models correctly locates the present location of the proton SAA is very significant. Knowledge of where the peak flux of the proton SAA is currently located is useful to the spacecraft designer to mitigate potential damage to systems and to mission planners.

### Acknowledgments

This work was supported by NASA's Earth Science Systems Office. J. Rose and C. Elliot of the Jet Propulsion Laboratory provided the data on TOPEX. The COBE data were provided through communications with T. Kelsall and B. Franz. Through a cooperative agreement with the University Research Foundation, outstanding services were provided, in particular, by Peter Messorre.

### References

<sup>1</sup>Van Allen, J. A., Ludwig, G. H., Ray, E. C., and McIlwain, C. E., "Observation of High Intensity Radiation by Satellites 1958 Alpha and Gamma,"

*Jet Propulsion*, Vol. 28, 1958, pp. 588-592.

<sup>2</sup>Gaffey, J. D., Jr., and Belitza, D., "National Space Science Data Center Trapped Radiation Models," *Journal of Spacecraft and Rockets*, Vol. 31, No. 2, 1994, pp. 166-176.

<sup>3</sup>Konradi, A., and Hardy, A. C., "Radiation Environment Models and the Atmospheric Cutoff," *Journal of Spacecraft and Rockets*, Vol. 24, 1987, p. 284.

<sup>4</sup>Lemaire, J., Daly, E. J., Vette, J. I., McIlwain, C. E., and McKenna-Lawlor, S., "Secular Variations in the Geometric Field and Calculations of Future Low Altitude Radiation Environments," *Proceedings of the ESA Workshop on Space Environment Analysis*, ESTEC, Noordwijk, The Netherlands, 1990, Sec. 5, Paper 17.

<sup>5</sup>Lauriente, M., Vampola, A. L., Inamti, P., and Bilitza, D., "Experimental Validation of Particle Model Drift Theories," *Journal of Spacecraft and Rockets*, Vol. 33, No. 2, 1996, pp. 250-254.

<sup>6</sup>Cain, J. C., Hendricks, S. J., Langel, R. A., and Hudson, W. V., "A Proposed Model for the International Geomagnetic Reference Field-1965," *Journal of Geomagnetism and Geoelectricity*, Vol. 19, 1967, pp. 335-355.

<sup>7</sup>Sawyer, D. M., and Vette, J., "Trapped Particle Environment for Solar Maximum and Solar Minimum (AP-8)," National Space Science Data Center, Rept. 76-06, Greenbelt, MD, 1976.

<sup>8</sup>Vampola, A. L., and Lauriente, M., "Using Cross-Correlations of SEUs and AP8 as a Diagnostic Tool," *Conference on the High Energy Radiation Background in Space*, Inst. of Electrical and Electronics Engineers, New York, 1998, pp. 118-123.

<sup>9</sup>Vampola, A. L., and Lauriente, M., "Solar Cycle Variations in the Inner Zone Proton Belt Configuration," *Conference on the High Energy Radiation Background in Space*, Inst. of Electrical and Electronics Engineers, New York, 1998, pp. 104-107.

<sup>10</sup>Huston, S. L., and Pfitzer, K. A., "A New Model for the Low Altitude Trapped Proton Environment," *IEEE Transactions on Nuclear Science*, Vol. 45, No. 6, 1998, pp. 2972-2978.

<sup>11</sup>Vampola, A. L., Lauriente, M., Huston, S., and Pfitzer, K., "Validating the New SEE Low Altitude Proton Model," *1997 Conference on the High Energy Radiation Background in Space*, Workshop Record, Inst. of Electrical and Electronics Engineers, New York, 1998, pp. 17-20.

<sup>12</sup>Edwards, D. J., and Hosken, R. W., "The TAOS/STEP Satellite," *Proceedings of the 9th Annual AIAA/Utah State University Conference on Small Satellites*, Vol. 9, Utah State Univ., Logan, UT, 1995, p. 4.

<sup>13</sup>Hosken, R., Koga, R., Wilson, B., Marcelli, J., and Laird, L., "Investigation of Non-Independent Single Event Upsets In The TAOS GVSC Static RAM," *IEEE Radiation Effects Data Workshop*, Inst. of Electrical and Electronics Engineers, New York, 1997, pp. 53-60.

<sup>14</sup>Hosken, R. W., and Wertz, J. R., "Microcosm Autonomous Navigation System On-Orbit Operation," *18th Annual Rocky Mountain Conference*, American Astronautical Society, 1995, p. 491-506.

A. C. Tribble  
Associate Editor